Journal of Biomolecular NMR **28:** 385–390, 2004.
KLUWER/ESCOM

Quantitation of rapid proton-deuteron amide exchange using hadamard spectroscopy

Catherine Bougault[a], Lianmei Feng[b], John Glushka[b], Eriks Kupče[c] & J.H. Prestegard[b,*]
[a]*Structural Biology Institute, CNRS, Grenoble, France;* [b]*Complex Carbohydrate Research Center, University of Georgia, Athens, GA, U.S.A.* [c]*Varian Associates, Palo Alto, CA, U.S.A.*

Received 14 October 2003; Accepted 20 October 2003

Key words: HSQC, ^{15}N, NMR, protein structure, ubiquitin

Abstract

The rates of amide proton exchange in protein backbones are very useful reporters of accessibility and structural stability of specific residues and secondary structure elements. Measurement by monitoring changes in intensity of cross-peaks in standard ^{15}N-^{1}H HSQC spectra as protons are replaced by solvent deuterons has become widely accepted. However, these methods are limited to relatively slow rates due to time limitations of the conventional 2D HSQC experiment. Here we show that a Hadamard encoded version of the HSQC, which relies on a multiplexed, frequency selective, excitation in the ^{15}N dimension, extends application to rates that are as much as an order of magnitude faster than those previously accessible.

The measurement of proton exchange rates at amide sites along the backbone of proteins provides insight into both structural and dynamic properties of these systems (Dempsey, 2001). The most widespread use has been in characterization of the stability of secondary elements. The rates in these cases are slow and measurement involves the base catalyzed exchange of protons for deuterons on occasional sampling of open states that are in equilibrium with the closed states of secondary structural elements. There are, however, reasons to monitor more rapid exchange processes. For example, there is substantial interest in using amide exchange to probe intermediates in protein folding pathways where secondary structure elements appear to be significantly less stable (Englander, 2000). There is also interest in rates of exchange at surfaces of proteins where rates can be very fast. Rates of exchange in these regions, in addition to amino acid sequence, depend on local environmental factors such as solvent accessibility, ionization states of nearby groups, and presence and absence of bound ligands (King et al., 2002; Mandell et al., 2001; McCallum et al., 2000). These latter factors can give important insight into protein function. In addition, one can imagine the use of exchange rates as an additional frequency dimension in multidimensional spectroscopy of proteins. All of the above provide motivation for exploring new methods of measuring amide exchange, particularly ones that extend measurements into regimes that have been hard to access. We present one such method here, measurement of proton to deuteron exchange using Hadamard encoding (Freeman and Kupce, 2003).

Methods for measurement of both very slow and very rapid exchange rates exist (Dempsey, 2001). At the very slow end simple monitoring of the loss of intensity in amide proton signals as a function of time after diluting a fully protonated protein sample in $^{2}H_2O$ usually suffices. Given the need to resolve and assign resonances, monitoring is usually done through cross-peaks of two-dimensional correlation spectra such as ^{15}N-^{1}H HSQC spectra. Measurements are limited by the sensitivity and minimum time for recording such spectra, but with modern NMR probes (including cryogenic and capillary probes) and reasonably soluble proteins (0.5 mM), exchange half times on the order of several minutes can be acquired. At

*To whom correspondence should be addressed. E-mail: jpresteg@ccrc.uga.edu

Table 1. Ubiquitin amide H/D exchange rate constants measured with Hadamard spectroscopy on a 48 h period at 25 °C and pH = 6.2 in 50 mM phosphate buffer[a]

Residue	k (min^{-1})	k (min^{-1})[c]	$T_{1/2}$ (min)[b]
Q2	>2.03E+00	1.82E+02	< 0.34E+00
I3	<3.83E-05	4.36E-04	> 1.81E+04
F4[d]	<3.63E-05	5.30E-04	>1.91E+04
V5[d]	<3.63E-05	7.11E-04	>1.91E+04
K6	6.93E-04	1.05E-02	1.00E+03
L8[d]	>1.68E+00		<0.41E+00
G10	>2.03E+00		<0.34E+00
K11[d]	1.32E-02		5.27E+01
T12	>2.03E+00	4.91E-01	< 0.34E+00
I13	1.63E-03	2.95E-03	4.24E+02
T14[d]	>1.68E+00		<0.41E+00
L15[d]	<3.63E-05	3.85E-01	>1.91E+04
V17[d]	<3.63E-05	7.97E-04	>1.91E+04
E18	3.54E-03		1.96E+02
E18[d]	4.94E-03		1.40E+02
S20	>2.03E+00		<0.34E+00
T22	3.08E-03	9.78E-01	2.25E+02
I23[d]	3.45E-04	1.13E-03	2.01E+03
N25[d]	1.19E-02	1.06E-01	5.84E+01
V26[d]	<3.63E-05	6.13E-05	>1.91E+04
K27	<3.83E-05		>1.81E+04
K27[d]	1.16E-05		5.94E+04
K29	<3.83E-05	2.82E-03	> 1.81E+04
K29[d]	<3.63E-05	2.82E-03	>1.91E+04
I30[d]	<3.63E-05	8.87E-05	>1.91E+04
D32[d]	1.40E-01	1.82E+00	4.96E+00
K33	5.46E-01		1.27E+00
E34[d]	4.80E-02		1.44E+01
G35	2.61E-01		2.66E+00
I36	1.46E-02	1.49E-01	4.74E+01
I36[d]	1.35E-02	1.49E-01	5.14E+01
D39[d]	>1.68E+00		<0.41E+00
Q40[d]	1.31E-01	5.54E-01	5.30E+00
Q41[d]	5.37E-02	1.18E-01	1.29E+01
R42	1.67E-02	6.15E-02	4.14E+01
F45[d]	6.69E-03	1.48E-02	1.04E+02
K48[d]	5.16E-02	3.81E-02	1.34E+01
Q49	>2.03E+00	1.49E+00	<0.34E+00
L50[d]	5.75E-03	4.08E-02	1.21E+02
E51	1.39E-01		4.97E+00
D52	>2.03E+00		<0.34E+00
R54	1.06E-02		6.57E+01
R54[d]	9.31E-03		7.44E+01
T55	9.99E-04	2.73E-02	6.94E+02
L56[d]	<3.63E-05	1.01E-03	>1.91E+04
S57[d]	1.59E-01	2.85E-01	4.36E+00
D58[d]	5.55E-02	4.58E-01	1.25E+01
I61	9.16E-03	1.05E-02	7.56E+01
I61[d]	1.28E-02	1.05E-02	5.42E+01
E62[d]	7.43E-02		9.33E+00
K63	>2.03E+00		<0.34E+00
K63[d]	>1.68E+00		<0.41E+00
S65	2.04E-01	9.40E-02	3.40E+00
T66[d]	1.74E-01		3.98E+00
L67	1.23E-02	3.60E-02	5.62E+01
H68[d]	7.88E-02	1.13E-01	8.80E+00
L69[d]	>1.68E+00	1.11E-02	<0.41E+00
V70[d]	1.44E-03	2.75E-03	4.81E+02
G76	>2.03E+00		<0.34E+00

[a]An error of 5% at rates near 1×10^{-3} estimated from analysis fits to decay curves for V70 and an error of 10% at rates near 1×10^{-2} estimated from analysis fits to decay curves for R42.
[b]$T_{1/2}$ is the half time for amide proton exchange, $T_{1/2} = \ln(2)/k$.
[c]k is back calculated from the protection factors in the paper by Pan and Briggs (1992).
[d]Exchange rate constants measured at 800 MHz; all others at 600 MHz. 800 MHz values are adjusted to pH = 6.2 from 6.0.

the fast end, selective perturbation of water proton magnetization in a protonated sample, followed by monitoring changes of crosspeaks as water protons exchange into amide proton sites, provides an effective method of measurement (Hernandez and LeMaster, 2003; Mori et al., 1997). Here the measurement range is limited by the spin relaxation time of water, restricting measurements to processes with half times shorter than a few seconds. Rates in the range between these limits, covering about two orders of magnitude, have been difficult to measure. The single scan 2D methods developed recently by Frydman et al. (2002) could potentially be used, but only for more concentrated samples (Pelupessy, 2003). Hadamard methods provide an alternate approach that offers an improvement in efficiency of HSQC collection that makes most of the missing range accessible on less concentrated samples.

Techniques based on Hadamard transform (HT) have been used in various types of spectroscopy for some time (Harwit, 1978; Griffiths, P., 1978). They are based on selective excitation and simple multiplexing principles to efficiently focus observation on known positions of spectral lines. In the case of an HSQC spectrum in which one intends to monitor cross-peak intensity as a function of time after dissolution in ^2H_2O one is usually in a situation where cross-peaks of interest, or those exhibiting most rapid exchange

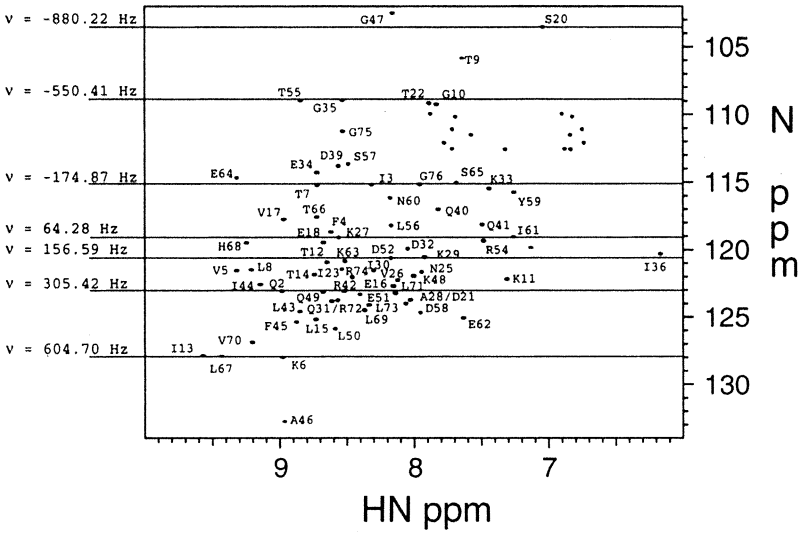

Figure 1. Conventional [^{1}H,^{15}N]-HSQC spectrum of human ubiquitin. The ^{15}N-labeled sample was purchased from Cambridge Isotope Laboratories (Andover, MA), and a 0.5 mM sample was prepared in 50 mM potassium phosphate buffer in H_2O/D_2O 5/95, pH=6.2. DSS (1mM) was used as internal standard for chemical shift calibration. Spectra were collected on a Varian Inova 600 spectrometer equipped with a cryogenic probe (Chiliprobe) with z-axis pulse field gradients using sweep widths of 6492.5 Hz and 2100 Hz respectively and using 2048 and 128 data points respectively in the direct ^{1}H dimension and the indirect ^{15}N dimension.

rates, fall within a small number of bands of nitrogen frequency. When the number of bands is limited, it is clearly more efficient to excite and observe directly these bands as opposed to executing a periodic excitation scheme as is done in a typical 2D HSQC. It is also well known that simultaneous observation of all bands in various combinations of sums and differences is more efficient than observation of one band at a time. Modern spectrometers are capable of generating selective excitation schemes in these sum and difference patterns and the HT provides a means of decoding the complex signals that result. Recently, there have been several descriptions of pulse sequences following principles of Hadamard encoding (Freeman and Kupce, 2003). We simply implement an HSQC sequence and specifically optimize it for amide exchange applications in what follows.

Application will be to human ubiquitin, 90% ^{15}N labeled in amide sites. Amide exchange in ubiquitin has been studied in the past by both NMR and mass spectrometric methods (Akashi et al., 1999; Pan and Briggs, 1992). The most comprehensive previous NMR work actually used amide to alpha proton cross-peaks in homonuclear COSY spectra on a 2.5 mM sample to follow deuterium for proton exchange (Pan and Briggs, 1992). By reducing the pH to 3.5 these workers slowed the faster exchange rates enough to allow observation with spectra requiring approximately 2 h. In the base catalyzed regime the pH change reduces rates by nearly three orders of magnitude from the rates we would observe at pH 6.2. More precisely, observed half times of 1 h at pH 3.5 are predicted to correspond to half times of 12 s at pH 6.2. However, a reduction in pH is not always compatible with protein stability and the need to characterize these systems under conditions where proteins normally function. In our case, a sample approximately 0.5 mM in ubiquitin was prepared in phosphate buffer at pH 6.2 and observed at 25 °C. Initially the sample was prepared in $^{1}H_2O$, a ^{1}H-^{15}N HSQC reference spectrum was run, and the sample was lyophilized. At time zero in the exchange rate study the sample was dissolved in $^{2}H_2O$ and transferred to the spectrometer for observation. Dissolution and transfer was done manually, limiting the first observation point to approximately 1 min, but we shall show that high quality HSQC data on more than 20 cross-peaks can be acquired in 40 s or less. This suggests an ability to span much of the missing time scale range mentioned above with future improvements in sample mixing and spectrometer loading procedures.

Figure 1 shows a conventional gradient sensitivity-enhanced [^{1}H,^{15}N]-HSQC spectrum of human ubiquitin. This spectrum was collected on the same 0.5 mM, pH 6.2, sample to be used in the HT NMR studies. Using a 600 MHz spectrometer equipped with

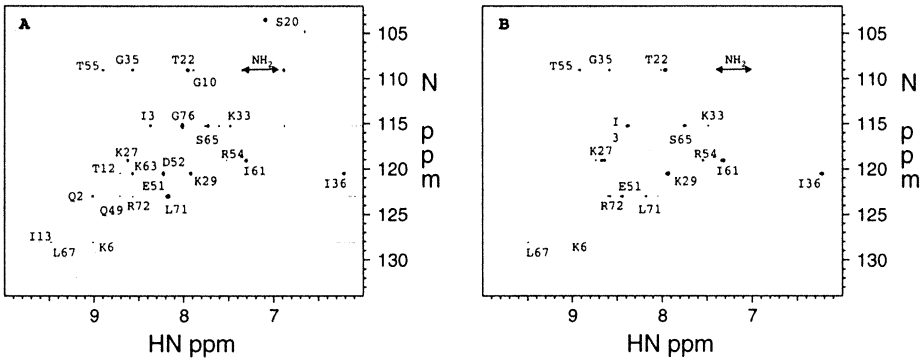

Figure 2. Reconstructed Hadamard [^{1}H,^{15}N]-HSQC spectra for ubiquitin. (A) Data in ^1H_2O collected with 128 t1 increments in 20 min. The sample was then lyophilized overnight and brought back to its initial volume with 99.9% ^2H_2O and immediately returned to the spectrometer for rapid collection of a series of Hadamard spectra. (B) First point after 1 min in ^2H_2O collected with 4 scans in 42 s.

a cold probe, it required approximately 21 min using 128 t1 time increments and 4 scans per increment, each one collected twice to achieve quadrature using the States-TPPI method. One observes 70 cross-peaks, a number in good agreement with that expected for this 8.6 kDa protein. With a collection time of this magnitude, and even sacrificing a factor of two in the signal to noise ratio, it would be impossible to obtain exchange rate data for sites with half times much less than 5 min. Yet, as stated above, we know that amide exchange rates extend from seconds to months. The Hadamard encoding allows one to focus on a subset of cross-peaks representing amides with exchange rates that include some from the more rapidly exchanging sites, and in so doing, greatly improve the efficiency of data acquisition at any given pH. Using the previously published NMR data, and accounting for pH differences, we were able to identify an appropriate set of peaks lying at 7 ^{15}N frequencies indicated by the lines drawn across Figure 1. The selected residues are S20, G35, G76, K27, D52, Q2 and K6. However, the selected frequencies (with a band width of 25 Hz) intersect a number of other cross-peaks allowing observation of 27 amide sites, or about 40% of all peaks. All of these peaks can be sampled with 8 Hadamard increments (combinations of the seven frequencies selected), in about 1/32 the time that was used in our conventional HSQC experiment. When scaled to equal total acquisition times the Hadamard experiment also shows a sensitivity advantage, but this is smaller and is not as important as the time savings for the application at hand.

Figure 2A shows the HT NMR spectrum of ubiquitin in ^1H_2O collected with 64 scans for each of the 8 increments in the Hadamard encoding matrix. Excitation of ^{15}N sites was achieved using combinations of 180° ('on') and 0° ('off') Gaussian pulses having 25 Hz bandwidths and representing correspondingly '+' and '−' elements in the Hadamard matrix, $\mathbf{H}_8$. The particular combinations vary in each increment of an $\mathbf{H}_8$ matrix that contains all 180° pulses in the first increment. Proton decoupling was achieved during the length of the encoding pulses (36 ms) with a WURST-2 decoupling scheme consisting of an even number of adiabatic pulses. Principles underlying the sequence used to collect the spectrum have been described in more detail in the literature (Kupce and Freeman, 2003). Figure 2B shows an equivalent spectrum taken 1.13 min after the addition of ^2H_2O to the lyophilized protonated sample using 4 scans per increment. This spectrum required 42 s. Data processing, including the Hadamard transform, was achieved using the nmrPipe software (Delaglio et al., 1995). Although it would be possible to present transformed data as seven one-dimensional traces, a 2D plot has been reconstructed, within nmrPipe, from the traces using Lorenzian lines in the indirect dimension. This allows a more direct comparison to the spectrum in Figure 1. Comparison of Figures 2A and 2B clearly demonstrates that the exchange is nearly complete for 9 resonances, even after 1 min. However, reductions in intensities of other peaks are easily quantified. For example, G35 has lost approximately $\frac{1}{2}$ its intensity in the same time interval. Similar spectra were collected at the following times: 2.05, 4, 6, 10, 20, 30, 45, 60, 120, 180, 240, 300, 360, 480, 720, 1440, 1800, 2748 min. To expand the set of cross-peaks that could be characterized a second sample was prepared and a second set of ^{15}N frequencies was selected (one overlapping the previous set to assess reproducibility). Similar data

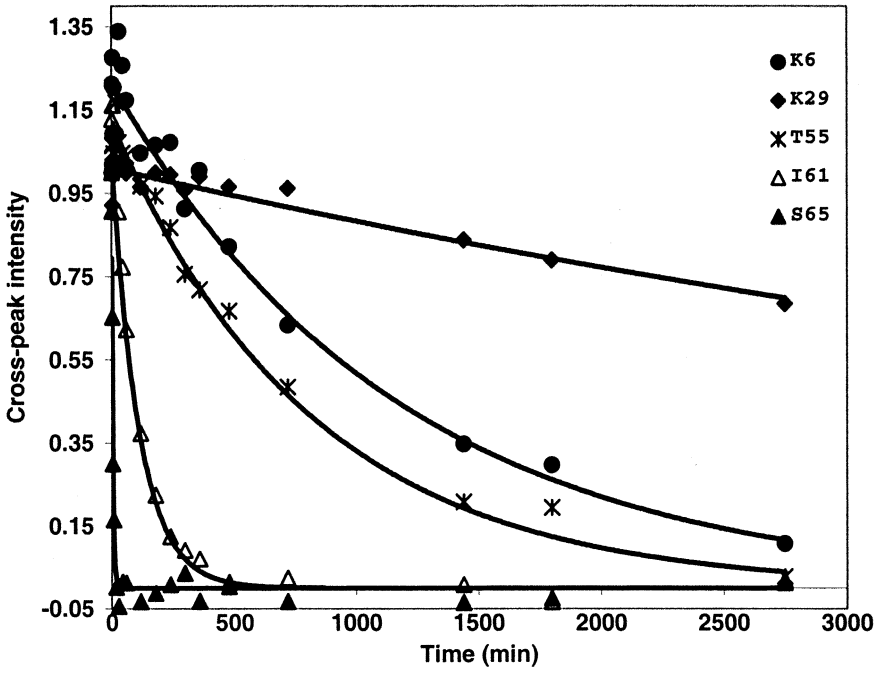

Figure 3. Cross-peak intensities measured as a function of time after Hadamard transform and 2D reconstruction for selected amide resonances. Lines are best fits to Equation 1.

collection procedures were used except that data were collected on an 800 MHz spectrometer equipped with a conventional triple resonance probe. The number of determined exchange rates could thus be extended to 52.

Figure 3 presents time courses for the decay of several representative cross-peaks. Peaks in spectra such as shown in Figure 2 were picked in nmrPipe and volumes were measured in each Hadamard spectrum. After normalization to the scaled peak intensities in the first spectrum, cross-peak intensities, $I(t)$, were plotted as a function of time. Decay rate constants were then extracted from these time courses using a Monte-Carlo procedure within nmrPipe. Equation 1 was used to include the effects of site-specific deuteration and residual ^1H_2O in the solution. The decays are clearly exponential and fit well to the equation.

$$I(t) = I_0(\exp(-kt) + \text{const}). \quad (1)$$

Table 1 reports measured exchange rates ranging from approximately 5×10^{-1} min^{-1} to 1×10^{-5} min^{-1} for ubiquitin at pH = 6.2; these correspond to half times from 1 min to more than 16 h. Longer half times are clearly present and could easily be measured by taking points at later times. Exchange rates as high as 1 per minute can thus be accurately determined on a sample that is approximately 0.5 mM using HT NMR. This extends by more than an order of magnitude the range of rates accessible by deuterium exchange NMR. The advantage of the Hadamard technique stems from the short time-frame necessary to collect data when the density of peaks is low or only a subset of peaks is of interest. In ubiquitin we are in principle interested in all rates. Rates for all amides in ubiquitin could not be collected in a single experiment, but the rates for approximately 75% of all amides could be collected in two experiments, while maintaining a substantial improvement in time required for the first point. Had we chosen to collect four or five experiments using three ^{15}N frequencies instead of 7, the time for the first point could have been reduced by another factor of two.

The precision of the data is quite high with the estimated errors for rates in the range of 1×10^{-3} min^{-1} being on the order of 5%. Rates derived also show reasonable agreement with previously published rates. A direct comparison with previous data is not straightforward, because these were collected at low pH and reported as protection factors (Pan and Briggs, 1992). However, if we assume no pH dependent structural change, correct for pH differences, and convert to exchange rates using equations available in the literature (Bai et al., 1993), we can make a semi-quantitative

comparison. These calculated rates are included in Table 1.

A correlation plot of log rates for residues measured in both sets gives an R squared value of 0.62. There are, however, a few significant outliers lowering the correlation; these may reflect interesting structural properties of the protein. The most pronounced outlier is a point for T22 that shows an unusual slowing of rates at the higher pH. Examination of the structure shows that T22 lies between two carboxylate terminated residues, D21 and E24 (both within 6Å of the T22 HN bond). It is likely that these proximate residues are uncharged at pH 3.5, but negatively charged at pH 6.2. This could locally decrease the hydroxide ion concentration needed for catalysis of exchange at the higher pH.

A more general point is that we have been able to measure our rates at a more physiologically relevant pH, even for some of the more rapidly exchanging sites. The utility of information on these more rapidly exchanging amide protons is yet to be fully demonstrated. However, we can point out that the more rapidly exchanging amides are on surface exposed residues in less structured loops. On examining the crystal structure (PDB code 1UBI), fifteen of sixteen residues with exchange rates greater than 0.1 min^{-1} are found to have greater than 5% of backbone atom surfaces solvent exposed as compared to only one of 11 of the residues having exchange rates less than 5 $\times$ 10^{-3} min^{-1} (Koradi et al., 1996). These surface exposed residues are ones whose environments (and exchange rates) are likely to be perturbed on ligand binding, protein–protein association, and changes in other environmental factors such as ionization states of nearby residues.

Acknowledgement

This work was supported by grants from the National Institutes of Health, GM033225 and RR005351.

References

Akashi, S., Naito, Y. and Takio, K. (1999) *Anal. Chem.*, **71**, 4974–4980.

Bai, Y.W., Milne, J.S., Mayne, L. and Englander, S.W. (1993) *Prot. Struct. Funct. Genet.*, **17**, 75–86.

Delaglio, F., Grzesiek, S., Vuister, G. W., Zhu, G., Pfeifer, J. and Bax, A. (1995) *J. Biomol. NMR*, **6**, 277–293.

Dempsey, C.E. (2001) *Prog. NMR Spectrosc.*, **39**, 135–170.

Englander, S.W. (2000) *Annu. Rev. Biophys. Biomol. Struct.*, **29**, 213–238.

Freeman, R. and Kupce, E. (2003) *J. Biomol. NMR*, **27**, 101–113.

Frydman, L., Scherf, T. and Lupulescu, T. (2002) *Proc. Nat. Acad. Sci. USA*, **99**, 15858–15863.

Harwit, M. (1978) In *Transform Techniques in Chemistry*, Griffiths, P. (Ed.), Plenum Press, New York, NY, pp. 173–183.

Hernandez, G. and LeMaster, D.M. (2003) *Magn. Reson. Chem.*, **41**, 699–702.

King, D., Lumpkin, M., Bergmann, C. and Orlando, R. (2002) *Rapid Commun. Mass. Spectrosc.*, **16**, 1569–1574.

Koradi, R., Billeter, M. and Wüthrich, K. (1996) *J. Mol. Graphics*, **14**, 51.

Kupce, E. and Freeman, R. (2003a) *J. Magn. Reson.*, **163**, 56–63.

Kupce, E. and Freeman, R. (2003b) *J. Biomol. NMR*, **25**, 349–354.

Mandell, J.G., Baerga-Ortiz, A., Akashi, S., Takio, K. and Komives, E.A. (2001) *J. Mol. Biol.*, **306**, 575–589.

McCallum, S.A., Hitchens, T.K., Torborg, C. and Rule, G.S. (2000) *Biochemistry*, **39**, 7343–7356.

Mori, S., Abeygunawardana, C., Berg, J.M. and vanZijl, P.C.M. (1997) *J. Am. Chem. Soc.*, **119**, 6844–6852.

Pan, Y.Q. and Briggs, M.S. (1992) *Biochemistry*, **31**, 11405–11412.

Pelupessy, P. (2003) *J. Am. Chem. Soc.*, **125**, 12345–13250.